1997

Atomic and electronic structures of neutral and charged boron and boron-rich clusters

J. Niu
Virginia Commonwealth University

B. K. Rao
Virginia Commonwealth University

P. Jena
Virginia Commonwealth University, pjena@vcu.edu

Niu, J., Rao, B. K., & Jena, P. Atomic and electronic structures of neutral and charged boron and boron-rich clusters. The Journal of Chemical Physics, 107, 132 (1997). Copyright © 1997 American Institute of Physics.

Atomic and electronic structures of neutral and charged boron and boron-rich clusters

J. Niu, B. K. Rao, and P. Jena
Physics Department, Virginia Commonwealth University, Richmond, Virginia 23284-2000

(Received 29 July 1996; accepted 28 March 1997)

Ab initio molecular orbital theory based on both density functional formalism and quantum chemical methods has been used to calculate the equilibrium geometries, binding energies, ionization potentials, fragmentation patterns, and electronic structures of neutral and charged boron clusters containing up to six atoms. Calculations have also been performed on restricted geometries for B_nX ($n=1,5,12$; X=Be, B, C) and B_{20} clusters to see if clusters can be designed so as to increase their stability. Energetics of doubly charged B_n^{++} clusters have also been studied to find the critical size for Coulomb explosion. The results are compared with existing experimental and theoretical data. © *1997 American Institute of Physics.* [S0021-9606(97)01525-0]

I. INTRODUCTION

The realization that atomic clusters constitute a new phase of matter has created considerable interest in the study of their structural and electronic properties.[1] In the past several years considerable progress has been made in our understanding of the evolution of equilibrium geometries, nature of bonding, cohesive energies and electronic structure of semi-conductors (mostly carbon and silicon), metal, and van der Waals clusters. However, the number of experimental and theoretical studies of boron clusters has been rather limited. This is surprising because boron exhibits some of the most interesting chemistry of all elements in the periodic table.[2] In addition, boron and boron-rich materials have important technological applications such as in explosives, refractory materials, high modulus fiber composites, stable chemical insulators, high temperature semiconductor devices, and thermoelectric power conversion.

Boron is isovalent with Al, yet the atomic and electronic structure of the two elements is entirely different. Al is a nearly free-electron metal where the valence electrons are delocalized and the solid phase is face centered cubic. Boron-rich solids, on the other hand, are composed of 12-atom clusters of boron having the structure of an icosahedron.[2] The electronic structure is characterized by three-center bonding, where three boron atoms share a common pool of charge. It is well known that in covalently bonded materials, the bonding charges are centered between two atoms. Thus the electronic structure of boron is intermediate between covalent and metallic bonding. This behavior renders boron-rich solids some of the most unusual properties. For example, boron-rich solids range from conducting materials ($B_{1-x}C_x$) to insulating materials ($B_{12}P_2$).

It is interesting to ask if the unique electronic structures of boron and boron-rich solids are prevalent even in the cluster phase. For example, consider the B_{20} cluster. Since boron is trivalent, and a dodecahedron is composed of pentagonal faces with each atom being three-fold coordinated, a covalently bonded B_{20} cluster could exhibit unusual stability like that of C_{60}. It has also been suggested[3] that $B_{36}N_{24}$ could have a fullerene structure and exhibit marked stability in analogy with C_{60}. However, in experiments where boron clusters were produced by laser ablation of hexagonal boron nitride, the existence of BN and B_2N as the only heteroatomic species was observed.[3] In contrast, an earlier experiment[4] had detected the existence of $B_nN_m^+$ for various combinations of n and m for $n=2-17$.

Only a handful of experimental investigations on pure boron clusters have been carried out in the past few years. Berkowitz and Chupka[5] were the first to study the mass spectra of B_{2-5} clusters. Recently, Hanley *et al.*[6] have measured the appearance potentials and fragmentation patterns by studying the collision-induced dissociation of boron cluster ions containing up to 13 atoms. They found that the stabilities generally increase with increasing cluster size, although there are large fluctuations. They also found that clusters smaller than six atoms fragment preferentially by losing a B^+, while for larger clusters, the charge remains on the B_{n-1}^+ fragment.

On the theoretical side, there have been very few studies. Langhoff and Bauschlicher[7] carried out a calculation of spectroscopic constants of B_2 by using an extensive Gaussian basis set and multireference configuration interaction (MRCI) approach. Hanley *et al.*[6] and Ray *et al.*[8] have calculated the relative stability of small B_n and B_n^+ clusters, as well as their fragmentation pattern and ionization potential. These calculations have been carried out by confining the structures to certain fixed geometries and optimizing the corresponding geometrical parameters. The atomic functions were represented by a less extensive set of Gaussians. *Ab initio* molecular dynamics studies[9] have also been reported for neutral boron clusters. However, no studies, theoretical or experimental, are available, to our knowledge, on the doubly charged boron clusters. It is interesting to ask if small doubly charged clusters of boron, due to their special chemistry, may be stable against Coulomb explosion.

In this paper we present a comprehensive study of the equilibrium geometries, vertical and adiabatic ionization potentials, and the fragmentation patterns of B_{2-6} clusters in neutral and singly charged states. The energetics and equilibrium geometries of B_n^{++} ($n=2-6$) provide insight into

 0021-9606/97/107(1)/132/9/$10.00

the role of boron's special chemistry on Coulomb explosion. We have also studied the stability of boron-rich clusters (B_nX; $n=1,5,12$; X=Be, C) to examine if they differ from the corresponding behavior in Al based clusters. Finally, the energetics of B_{20} confined to a dodecahedral shape was studied to see if two-center bonding between boron atoms is preferred in the cluster, thus enhancing its relative stability. These calculations are based on *ab initio* self consistent field molecular orbital theory using both density functional and quantum chemical approaches. In Sec. II we provide a brief discussion of our methods. The results obtained using different levels of theory are presented in Sec. III and summarized in Sec. IV.

TABLE I. Basis set for boron.

S 7 1.0		P 4 1.0		D 1 0.9	
2788.41	0.001 288	11.3413	0.017 988	1.488	1.0
419.039	0.009 835	2.435 99	0.110 343		
96.4683	0.047 648	0.683 58	0.383 072		
28.0694	0.160 069	0.213 36	0.647 895		
9.37597	0.364 984				
3.406 23	0.433 582	P 1 1.17			
1.305 66	0.140 082				
		0.200 114	1.0		
S 2 1.0					
3.406 23	−.17933				
0.324 48	1.062 594				
S 1 0.9					
0.102 19	1.0				

II. THEORETICAL METHODS

For calculation of the total energies, electronic structure, and equilibrium geometries, we have used the Hartree–Fock method, followed by a correlation correction though Möller–Plesset fourth order perturbation theory (MP4).[10] This approach is computationally demanding and has been used to study small clusters only. On the other hand, the density functional method with generalized gradient approximation (GGA)[11] enables one to treat larger clusters not possible within the traditional quantum chemistry formalism. This formulation has been shown[11] to yield accurate results when compared to experiments in bulk metallic systems. However, a quantitative comparison between GGA and quantum chemical approach in bulk systems is not feasible. Such comparisons can be readily made in small atomic clusters. Here we have used both the methods to study clusters of up to six boron atoms. In the density functional approach we have used the GGA under the B3LYP scheme.[12] For all calculations, the GAUSSIAN 94 software[12] has been used. We have made use of the same Gaussian basis functions in both the approaches. For studies of boron-rich clusters (B_nX) ($n=1,5,12$; X=Be, B, C), only the density functional approach has been used.

The results also depend on the choice of basis sets. While very extensive basis function containing up to f orbitals, as used by Langhoff and Bauschlicher,[7] can yield quantitatively accurate results, it cannot be used for a large variety of systems, as studied here. On the other hand, reliable theoretical results can be obtained with less extensive basis sets. We have used $(10s,5p,1d/3s,2p,1d)$ basis functions for boron (see Table I) and the 6-311G** basis $(11s,5p,1d/4s,3p,1d)$ (Ref. 12) for both beryllium and carbon atoms.

In order to assess the accuracy of the basis functions, we have computed the total energy and ionization potential of C and B atoms as well as the preferred spin multiplicity, binding energies, bond lengths, and adiabatic ionization potentials of the respective dimers. These results, obtained at the HF-MP4 (SDTQ) and B3LYP levels of theory, are presented in Table II and compared with available experiment.[13] Note that the agreement between the experiment and both levels of theory is very good indeed. This provides confidence not only on the levels of theory, but also on the choice of the basis sets. In the following section we discuss the results on neutral and charged boron and boron-rich clusters separately.

III. RESULTS

Using the theoretical procedure outlined in the previous section, our first task has been to determine the equilibrium geometries of clusters and their corresponding binding energies and electronic structures. We have used the method of steepest descent for this purpose. The cluster was initially constructed by placing the atoms at random locations and calculating the total energy. The forces at the atomic sites were computed by using the numerical gradient technique and the atoms were moved to a new location along the path dictated by the steepest descent method. The process was continued until the forces vanished at every atomic site. It should be emphasized that during this process the cluster could be trapped at various metastable minima that exist on the potential energy hyper surface. It was, therefore, necessary to repeat the above process with different initial geometries. Harmonic vibrational frequencies were calculated at the minimum energy configurations to ensure that the minimization procedure had worked properly. It should also be emphasized that one needs to optimize the spin multiplicities of the clusters as well. In what follows, we only quote the results relevant to the most stable geometries and spin multiplicities for B_n ($n\leqslant 6$) clusters. For clusters containing 13 atoms and larger, the optimization procedure has been limited in scope and will be discussed as appropriate.

A. Neutral boron clusters

In Fig. 1 we present the equilibrium geometries as well as the geometries of some isomers of B_{2-6} clusters calculated using the MP4 level of theory. Results for most of these geometries were also tested out using the GGA level of theory. The corresponding bond distances and bond angles are given in Table III. The preferred spin multiplicity and total energies (E_n) are given in Table IV. The binding energy E_b of a cluster of n atoms is calculated from the equation,

$$E_b(n)=-[E(n)-nE_0], \tag{1}$$

TABLE II. Testing the accuracy of the basis functions using different levels of theory.

		Binding energy (eV)			Bond length (Å)			I.P. (eV)		
System	Multiplicity	MP4	B3LYP	Expt.	MP4	B3LYP	Expt.	MP4	B3LYP	Expt.
B	2							8.25	8.295	8.298
C	3							11.04	12.12	11.26
B_2	3	2.85	2.91	2.833±0.238	1.55	1.56	1.59	10.16	9.81	10.4

where E_0 is the energy of the free atom. These are also listed in Table IV for both levels of theory.

Before commenting on the individual geometries and their evolution, we want to compare the results obtained using MP4 and B3LYP techniques. Note that the equilibrium geometries (with the exception of B_5) and spin multiplicities of clusters using both the methods agree very well with each other wherever comparisons were made. The geometrical parameters (bond lengths and bond angles) and the binding energies are also in good agreement with each other. Systematic increase in binding energy as a function of the cluster size is observed in both the methods. This can be clearly seen from Fig. 2. Note that unlike alkali metal clusters, there are no magic numbers (i.e., clusters with unusual stability) in B_n clusters in the size range studied.

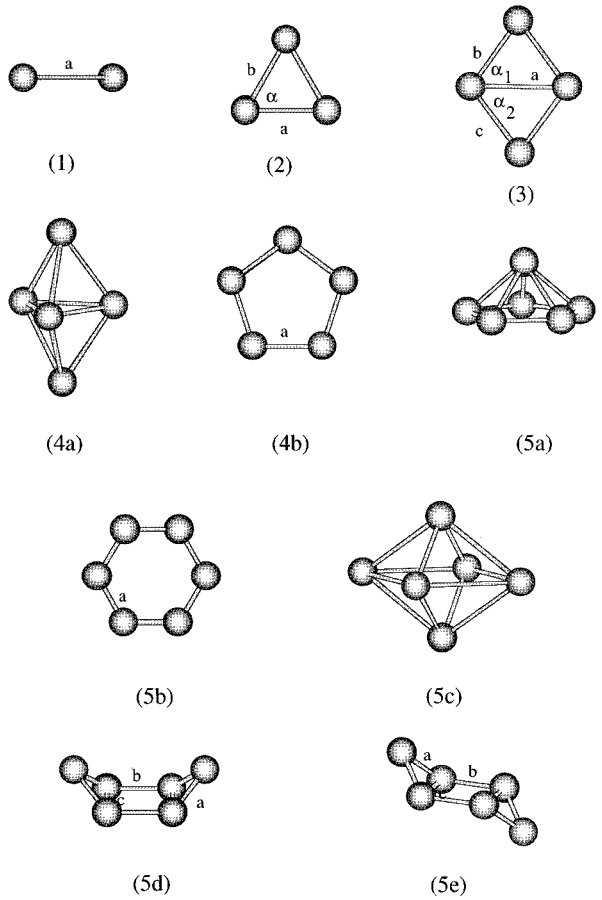

FIG. 1. Equilibrium geometries and geometries of isomers of some neutral B_n $(2 \leqslant n \leqslant 6)$ clusters.

We now discuss individual geometries. B_2 is the most theoretically studied cluster. Although very early calculations[14] of B_2 predicted the ground state to be in a spin quintet state, later calculations of Dupuis and Liu[15] and Langhoff and Bauschlicher[7] have conclusively shown that the ground state is a spin triplet—in agreement with the experiment.[16] Our results based upon both MP4 and B3LYP also yield the ground state of B_2 to be spin triplet. The bond length and binding energy, $E_b(n)$ of B_2 computed by Langhoff and Bauschlicher[7] using up to f and g orbitals in the basis set are, respectively, 1.60 Å and 2.78 eV. Our results at the MP4 level of theory for these quantities are 1.55 Å and 2.85 eV. This agreement further proves that the basis set we have chosen is adequate to obtain numerically reliable results on larger clusters.

The structure of B_3 is an equilateral triangle with a binding energy/atom $[E_b(n)/n]$ of 2.82 eV and bond length 1.52 Å at the MP4 level of theory. This is in agreement with the results obtained by Ray *et al.*[8] as well as by Hanley *et al.*[6] Our results, however, differ significantly from those of Ray *et al.* for B_4. These authors found B_4 to be a linear chain with a binding energy of 5.02 eV/atom. This is significantly higher than the 3.02 eV/atom binding energy/atom these authors have calculated for B_3. The equilibrium structure for B_4 in our calculations is a rhombus with a binding energy that is only 0.8 eV per atom higher than the corresponding B_3 binding energy. This important discrepancy can only be attributed to a less extensive choice of the basis functions (3-21G*) made by Ray *et al.*,[8] as we both use the MP4 level of theory. It should be noted that Hanley *et al.*[6] did find B_4 to be a rhombus. There is only a marginal difference in the bond length and angle between their and our calculations. We also agree with the ground state multiplicity (singlet) of B_4 as obtained by these authors. Note that the basis function (6-31G*) used by Hanley *et al.*,[6] although not as good as the one used here, is superior to that used by Ray *et al.*[8]

For the B_5 we have identified two isomers among which the triangular bipyramid is the most stable structure using the MP4 theory. The bond distance is 1.59 Å, which is very close to the values in previous structures. However, the B3LYP predicts the pentagonal structure to be the preferred geometry of B_5, although by a small margin. Note that this is the only structure where the B3LYP result is at variance with the MP4 result. The equilibrium structure of B_6 is a pentagonal pyramid. This is particularly interesting since the number of bonds in an octahedral structure, Fig. 1 (5c), is 12 while it is only 10 in the pentagonal pyramid structure. As Table IV shows, the energy of B_6 in the octahedral structure is 2 eV

TABLE III. Geometrical parameters for neutral B_n clusters (see Fig. 1). For geometries 4(a), 5(a), 5(c), a is the distance from the center of the horizontal plane to the atoms in the plane, and b is the height of the apex atoms from this point. α's are the angles between two lines in the same plane and β's are the dihedral angles between two planes.

Type of clusters	Geometry	Bond lengths (Å)		Bond angles (°)	
		MP4	B3LYP	MP4	B3LYP
B_2	Fig. 1-(1)	$a=1.55$	$a=1.56$		
B_3	Fig. 1-(2)	$a=1.52$, $b=1.52$	$a=1.52$, $b=1.52$	$\alpha=60.0$	$\alpha=60.0$
B_4	Fig. 1-(3)	$a=1.79$, $b=1.51$, $c=1.51$	$a=1.82$, $b=1.51$, $c=1.51$	$\alpha_1=53.6$, $\alpha_2=53.6$, $\beta=180.0$	$\alpha_1=52.8$, $\alpha_2=52.8$, $\beta=180.0$
	Fig. 1-(4a)	$a=1.09$, $b=1.16$	$a=1.09$, $b=1.16$		
B_5	Fig. 1-(4b)	$a=1.53$	$a=1.58$		
	Fig. 1-(5a)	$a=1.39$, $b=0.89$	$a=1.37$, $b=0.92$		
	Fig. 1-(5b)	$a=1.52$	$a=1.52$		
B_6	Fig. 1-(5c)	$a=1.36$, $b=0.98$			
	Fig. 1-(5d)	$a=1.49$, $b=4.63$, $c=1.57$		$\beta=90.1$	
	Fig. 1-(5e)	$a=1.53$, $b=3.00$, $c=1.60$		$\beta=84.1$	

above the ground state structure. The ''boat'' and the ''chair'' forms {see Fig. 1 [(5d) and (5e)]} are also of higher energy. This provides a signature of the special electronic structure of boron. If the bonding in B_n clusters would have been a two-centered covalent bond, the octahedral structure would have been the ground state. It is also evident that the seed for an icosahedric growth pattern is shown at the B_6 cluster stage. We can conclude that the special chemistry that governs the electronic structure of boron-rich solids is also present in small boron clusters.

B. Singly charged boron clusters

As an electron is removed from a cluster, the redistribution of charges causes the neutral structure to relax. The difference in the total energy between the neutral and cationic cluster in their respective ground states is the adiabatic ionization potential and has been measured by Hanely *et al.*[6] for B_{2-13} clusters. They have also observed that the fragmentation of B_n^+ clusters for $n<6$ proceeds by the emission of a B^+ atom, while in larger clusters the charge resides on the B_{n-1}^+ fragment.

We have optimized the geometries of B_n^+ ($n\leqslant 6$) clusters both at the MP4 and the B3LYP level of theory. Both methods, once again, yield identical geometries and spin multiplicities as in the case of the neutral clusters. These are presented in Fig. 3. The relevant geometrical parameters are tabulated in Table V. First, we compare the structures of neutral and corresponding cationic clusters. There is very little change among the geometries of neutral and charged dimers, trimers, and tetramers. Significant changes, however, occur in B_5 and B_6 clusters when an electron is removed. The planar structures are preferred for the positively charged clusters. The primary B–B bond, however, remains very close to that in the neutral clusters in all cases.

In Table VI we compare the total energy and the binding energy/atom $[E_b^+(n)/n]$ of B_n^+ clusters obtained using both the theoretical methods. The binding energy of singly

TABLE IV. Energetics and preferred spin multiplicities of neutral B_n clusters using MP4 and B3LYP theories. See Fig. 1 for corresponding geometries. For B_5 and B_6 clusters, the binding energy/atom is computed only for ground state structures.

Compound	Multiplicity		Geometry	Total energy, a.u.		Binding energy/atom, eV	
	MP4	B3LYP		MP4	B3LYP	MP4	B3LYP
B	2	2	/	−24.5487	−24.6398	/	/
B_2	3	3	Fig. 1-(1)	−49.2022	−49.3866	1.43	1.45
B_3	2	2	Fig. 1-(2)	−73.9567	−74.2669	2.82	3.15
B_4	1	1	Fig. 1-(3)	−98.7271	−99.1168	3.62	3.79
			Fig. 1-(4a)	−123.4108	−123.8438	3.63	
B_5	2	2	Fig. 1-(4b)	−123.3697	−123.8731		3.67
			Fig. 1-(5a)	−148.0944	−148.7722	3.64	4.23
			Fig. 1-(5b)	−148.0298	−148.6512		
B_6	1	1	Fig. 1-(5c)	−148.0199			
			Fig. 1-(5d)	−148.0445			
			Fig. 1-(5e)	−148.0199			

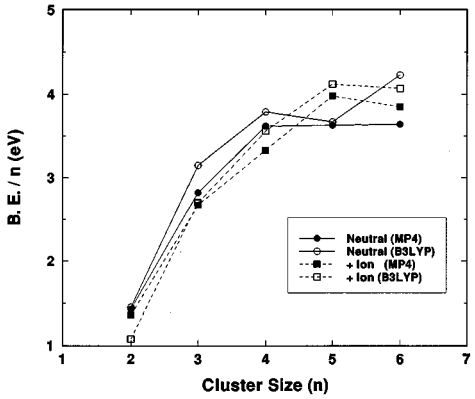

FIG. 2. Comparison of the binding energy/atom, $[E_b(n)/n]$, for neutral and charged B_n clusters calculated using MP4 and B3LYP theories.

charged clusters, $E_b^+(n)$ is calculated by using the equation

$$E_b^+(n) = -[E^+(n) - (n-1)E_0 - E_0^+], \tag{2}$$

where $E^+(n)$ and E_0^+ are, respectively, the total energies of the B_n^+ and B^+ in their ground state configurations. Note that both MP4 and B3LYP methods provide the same systematic variation, namely a monotonic rise with cluster size (see Fig. 2). On the contrary, in charged alkali metal clusters, these energies fluctuate with size.

The adiabatic potentials have been calculated by taking the difference between the ground state energies of neutral and positively charged clusters. These values obtained using the MP4 and B3LYP methods are compared with experimental results in Fig. 4. Note that unlike the binding energies in Fig. 2, the adiabatic potentials vary monotonically with size. Although our calculated values at both levels of theory are closer to the experiment than those calculated by Hanley *et al.*,[6] the agreement is far from perfect.

We next discuss the fragmentation of singly charged B_n^+ clusters. We only deal with binary fragmentation. There are two possible channels: $B_n^+ \rightarrow B_m^+ + B_{n-m}$ or $B_n^+ \rightarrow B_m + B_{n-m}^+$. The simplest way to examine this is to calculate the dissociation energies,

$$\Delta E_{nm}^+ = \begin{bmatrix} [E(m) + E^+(n-m)] - E^+(n) \\ \text{or} \\ [E^+(m) + E(n-m)] - E^+(n) \end{bmatrix}. \tag{3}$$

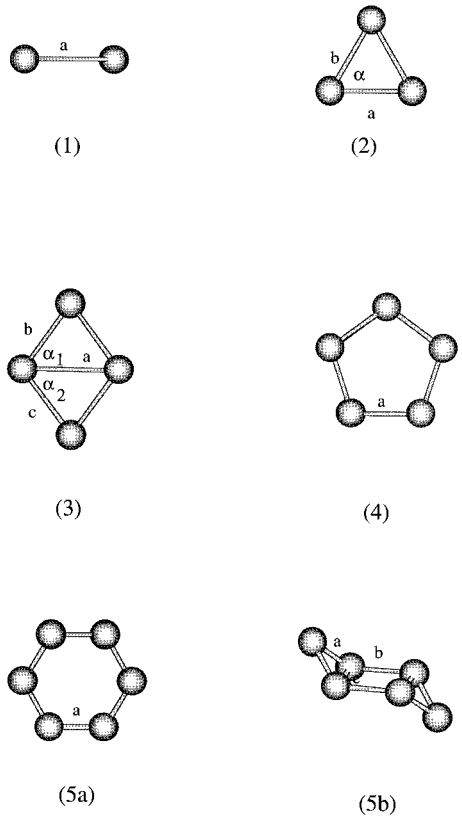

FIG. 3. The equilibrium geometries of B_n^+ clusters.

We compare the dissociation energies for different channels with experiment as well as the calculated values of Hanley *et al.*[6] in Table VII. The preferred channel is considered as the one for which ΔE^+ is minimum. In practice, the energy barriers separating the two fragments can also play an important role in the dissociation of the charged clusters. Such calculations have not been performed here. From the energetics in Table VII we see that the preferred channel is the emission of a B^+ ion for B_2^+ to B_5^+ clusters. For B_6^+ clusters, the preferred channel is the emission of a neutral boron atom. This trend is in agreement with experiment. However, our calculated dissociation energies (see Fig. 5) for the preferred channels, although following experimental systematics, do not agree quantitatively with experiment.[6]

TABLE V. Geometrical parameters for B_n^+ clusters (see Fig. 3). The notations for the figures are as given in Table III.

		Bond lengths (Å)		Bond angles (°)	
Type of clusters	Geometry	MP4	B3LYP	MP4	B3LYP
B_2^+	Fig. 3-(1)	$a=1.75$	$a=1.80$		
B_3^+	Fig. 3-(2)	$a=1.60,\ b=1.60$	$a=1.55,\ b=1.55$	$\alpha=60.0$	$\alpha=60.0$
B_4^+	Fig. 3-(3)	$a=1.98,\ b=1.55,\ c=1.55$	$a=2.00,\ b=1.54,\ c=1.54$	$\alpha_1=50.5,\ \alpha_2=50.5,\ \beta=180.0$	$\alpha_1=49.5,\ \alpha_2=49.5,\ \beta=180.0$
B_5^+	Fig. 3-(4)	$a=1.57$	$a=1.54$		
	Fig. 3-(5a)	$a=1.55$	$a=1.54$		
B_6^+	Fig. 3-(5b)	$a=1.67,\ b=1.60,\ c=1.69$	$a=1.64,\ b=1.65,\ c=1.67$	$\beta_1=149.2,\ \beta_2=149.2$	$\beta_1=110.1,\ \beta_2=110.1$

TABLE VI. Energetics for singly charged boron clusters, B_n^+ $(n=1-6)$.

	Multiplicity			Total energy, a.u.		Binding energy/atom, eV	
Clusters	MP4	B3LYP	Geometry	MP4	B3LYP	MP4	B3LYP
B_1^+	1	1	/	−24.2456	−24.3348	/	/
B_2^+	2	2	Fig. 3-(1)	−48.8941	−49.0540	1.36	1.08
B_3^+	1	1	Fig. 3-(2)	−73.6379	−73.9121	2.67	2.70
B_4^+	2	2	Fig. 3-(3)	−98.3815	−98.7779	3.33	3.56
B_5^+	1	1	Fig. 3-(4)	−123.1712	−123.6511	3.98	4.12
			Fig. 3-(5a)	−147.8376	−148.4326	3.85	4.07
B_6^+	2	2	Fig. 3-(5b)	−147.7578	−148.3328		

C. Doubly charged boron clusters

As a cluster is doubly ionized, the added repulsion between the two positive charges tends to destabilize the cluster. This destabilization force is the strongest for the smallest clusters. The smaller clusters usually spontaneously fragment unless there is an energy barrier that can protect the cluster against such a fate. This phenomenon is known as Coulomb explosion[17] and has been extensively studied in metal clusters. The critical size for Coulomb explosion increases with the increasing level of ionization. It has been shown theoretically[18] and verified experimentally[19] that some of the doubly charged metal dimers could be metastable and the electronic structure could play an important role in determining the metastability.

To our knowledge, no experimental or theoretical work on doubly charged B_n clusters is yet available. Since the chemistry of B_n clusters and solids is rather special, we have investigated the energetics and geometries of B_n^{++} clusters $(n\leqslant 6)$ using MP4 theory. In Fig. 6 we give the equilibrium geometries. The corresponding geometrical parameters are given in Table VIII. Note that unlike the singly charged clusters, the doubly charged clusters are all linear chains. However, the length of the bonds in the clusters remain almost unaltered from the neutral dimer value. The innermost bonds are slightly stretched as the excess charge mostly resides at the end atoms.

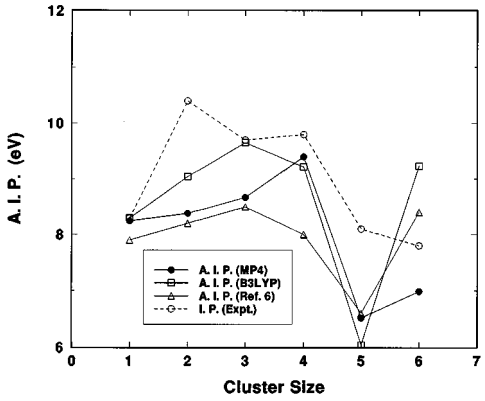

FIG. 4. Comparison of the experimental adiabatic ionization potentials of B_n clusters with those calculated using MP4 and B3LYP theories and other calculations (Ref. 6).

What is more unique about B_n^{++} clusters compared to other doubly charged clusters is their stability. To analyze these we have calculated the binding energy of the B_n^{++} cluster using the relation: $E_b^{++}(n)=[2E(B^+)+(n-2)\times E(B)-E(B_n^{++})]$. In Table IX we give the total energies, binding energies, and spin multiplicities of B_n^{++} clusters using the MP4 method. We find that B_2^{++} and B_3^{++} are unstable against fragmentation, as indicated by negative value of $E_b^{++}(n)$, while the larger B_n^{++} $(n\geqslant 4)$ clusters are stable against dissociation into individual ions and neutral atoms.

We have also checked to see if B_n^{++} is stable against any one of the two fragmentation channels: $B_m^+ + B_{n-m}^+$ and $B_m^{++} + B_{n-m}$. This is done by calculating the dissociation energy using the equations:

$$\Delta E_{nm}^{++} = E(B_n^{++}) - [E(B_m^+) + E(B_{n-m}^+)],$$
$$\Delta \widetilde{E}_{nm}^{++} = E(B_n^{++}) - [E(B_{n-m}) + E(B_m^{++})]. \quad (4)$$

A negative value of ΔE_{nm}^{++} or $\Delta \widetilde{E}_{nm}^{++}$ for any value of n and m means that fragmentation in that channel is *not* preferred. If ΔE_{nm}^{++} and $\Delta \widetilde{E}_{nm}^{++}$ are both negative for all possible values of m, we can conclude that B_n^{++} cluster could be stable against Coulomb explosion. The critical size for Coulomb explosion corresponds to the smallest value of n for which the above statement holds. Using the total energies of B_n, B_n^+, and B_n^{++} clusters given in Tables IV, VI, and IX at the MP4 level of theory, we find that none of the doubly charged clusters studied has reached the critical size for Coulomb explosion. This argument does not take into account the fact that energy barriers, as the fragments separate, may have an important influence on the critical size for Coulomb explosion observed experimentally. For example, in some transition metal clusters, doubly charged dimers have been observed,[19] even though ΔE_{nm}^{++} is negative.[18] Study of such energy barriers and experiments on the critical size for B_n^{++} clusters should yield interesting results.

D. Compound clusters of boron

The electronic structure and stability of clusters can be significantly altered by introducing impurities. As mentioned earlier, the structure of $B_{n-x}C_x$ solids is composed of B_{12} icosahedra connected by C-atoms, ie., the C-atoms reside outside the icosahedric cage.[2] It was demonstrated[20] that $Al_{12}C$, with carbon occupying the central site of an icosahe-

TABLE VII. Dissociation energies of B_n^+ clusters for different channels using MP4 and B3LYP theory.

Cluster	Dissociation channels	D. E. of this work, eV		D. E. of Hanley's work (Ref. 6), eV	D. E. of experiment, eV
		MP4	B3LYP		
B_2^+	$B_2^+ \Rightarrow B^+ + B$	2.715	2.150	0.7	0.8±0.6
	$B_3^+ \Rightarrow B^+ + B_2$	5.171	5.187	1.1	2.3±0.6
B_3^+	$B_3^+ \Rightarrow B_2^+ + B$	5.307	5.938	2.0	4.3±0.7
	$B_4^+ \Rightarrow B^2 + B_3$	4.874	4.793	1.2	2.4±0.6
B_4^+	$B_4^+ \Rightarrow B_2^+ + B_2$	7.757	9.175	3.2	/
	$B_4^+ \Rightarrow B_3^+ + B$	5.301	6.147	2.8	8.0±0.1.5
B_5^+	$B_5^+ \Rightarrow B^+ + B_4$	5.399	5.426	2.0	3.6±0.6
	$B_5^+ \Rightarrow B_2^+ + B_3$	8.715	8.981	/	/
	$B_5^+ \Rightarrow B_3^+ + B_2$	9.006	9.585	/	/
	$B_5^+ \Rightarrow B_4^+ + B$	6.555	6.348	/	7.1±0.6
	$B_6^+ \Rightarrow B^+ + B_5$	4.929	6.112	/	3.2±0.7
	$B_6^+ \Rightarrow B_2^+ + B_4$	5.886	7.121	/	/
B_6^+	$B_6^+ \Rightarrow B_3^+ + B_3$	6.610	6.898	/	/
	$B_6^+ \Rightarrow B_4^+ + B_2$	6.906	7.292	/	/
	$B_6^+ \Rightarrow B_5^+ + B$	3.201	3.854	2.2	2.7±0.6

dron, is far more stable than Al_{13}. This stability is partly derived from the fact that $Al_{12}C$ has 40 valence electrons that are enough to close the outermost electronic shells. Since boron is isoelectronic with aluminum, one wonders if $B_{12}C$ with C occupying the central site can show enhanced stability.

The binding energy of a compound cluster B_nX is defined as

$$\tilde{E}_b = E(X) + nE(B) - E(B_nX). \tag{5}$$

The geometries of B_nX clusters are given in Figures 7(a) and 7(b), respectively. The corresponding bond lengths, total energies, binding energies, spin multiplicity, and Mulliken charges are given in Table X. We note that out of the three dimers BBe, B_2, and BC, BBe is the least bound, while the binding energy of BC is larger than that of B_2. Be is a closed shell atom and its weak interaction with the B atom is understandable. However, this changes as we go to larger clusters. For example, the binding energy of B_5Be is only marginally smaller than that of B_5B or B_5C. In $B_{12}X$ clusters, note that $B_{12}Be$ is more strongly bound than either $B_{12}B$ or $B_{12}C$. This is particularly striking since the number of valence electrons in $B_{12}Be$ is 38 while that in $B_{12}C$ is 40. We recall that $Al_{12}C$ has a binding energy that is 4.4 eV larger[20] than that of Al_{13}. This is due to the fact that 40 electrons correspond to closed electronic shells in an otherwise jellium cluster. Thus $B_{12}C$ does not behave like $Al_{12}C$. This is further

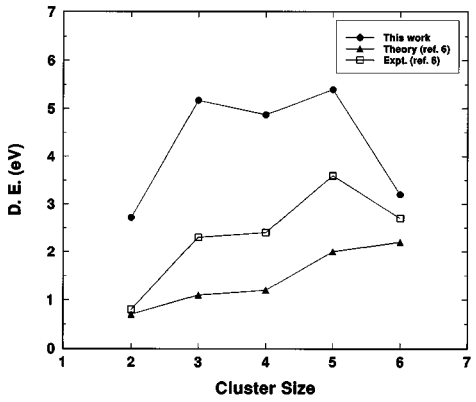

FIG. 5. Comparison of the preferred dissociation channels of B_n^+ clusters calculated using MP4 level of theory with the experimental and other theoretical works (Ref. 6).

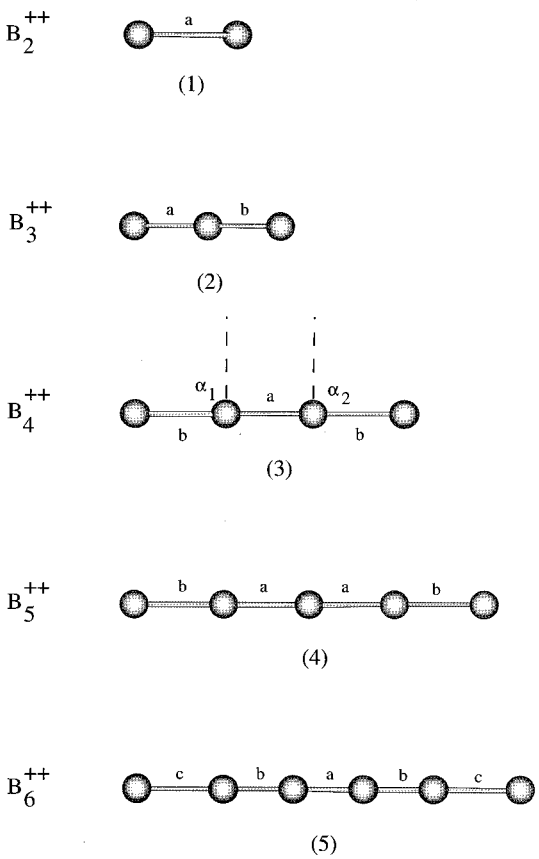

FIG. 6. Preferred geometries of B_n^{++} clusters.

TABLE VIII. Geometrical parameters for B_n^{++} clusters (see Fig. 6).

Type of clusters	Geometry	Bond lengths (Å)	Bond angles (°)
B_2^{++}	Fig. 6-(1)	$a=1.54$	
B_3^{++}	Fig. 6-(2)	$a=1.60,\ b=1.60$	
B_4^{++}	Fig. 6-(3)	$a=1.59,\ b=1.50$	$\alpha_1=89.6,\ \alpha_2=89.6$
B_5^{++}	Fig. 6-(4)	$a=1.58,\ b=1.50$	
B_6^{++}	Fig. 6-(5)	$a=1.53,\ b=1.67,\ c=2.15$	

ther indication that the electronic structure of boron clusters is different from its isoelectronic aluminum clusters, just as is the case with the bulk.

Further insight into the electronic structure of boron-rich clusters can be obtained by examining the Mulliken charge distribution in Table X. Note that the net charge on the central B in B_{13} icosahedron is negative, as it is on the central C and Be site in $B_{12}X$ cluster. The magnitude of the charge transfer increases as the central atom changes from C to Be. This is consistent with the increase in the binding energy.

Finally, we discuss the stability of B_{20}. This structure was confined to the dodecahedral shape (see Fig. 8) and the bond distance was optimized. The objective was to see if two-center bonding can be important in boron clusters. The binding energy/atom of B_{20} is found to be 5.56 eV, which is only marginally larger than that in B_{12}. Since the general tendency of binding energy is to increase with size, this marginal increase is not indicative of any magical stability of B_{20}. In other words, B_{20} may not constitute the smallest structure that could resemble a fullerene. We wish to emphasize that the studies of the relative stabilities of compound boron clusters carried out in this section have made use of restricted geometries. For example, the equilibrium structure of B_{13} cannot be an icosahedron (with the central site occupied), as it is energetically unstable compared to an icosahedric B_{12} cluster (icosahedron with the central site vacant) plus an isolated boron atom.

IV. CONCLUSIONS

The energetics and atomic and electronic structure of neutral and charged boron and boron-rich clusters have been studied using self consistent molecular orbital theory and two levels of approximation for the exchange and correlation potential. The results based on generalized gradient approximation agree well with those based on the Hartree–Fock-Möller–Plesset method. A number of conclusions are made. (1) The energetics do not reveal the existence of any magic number, as is well known for alkali metal clusters. (2) The nearest neighbor distance in clusters does not differ significantly from the dimer bond length. This is in contrast with the results in metallic or covalent systems. (3) The nature of

TABLE IX. Energetics and preferred spin multiplicities of B_n^{++} ($n=1-6$) clusters.

Compound	Multiplicity	Geometry	Total energy, a.u.	Binding energy, eV
B_1^{++}	2	/	−23.1461	/
B_2^{++}	1	Fig. 6-(1)	−48.1069	−10.45
B_3^{++}	2	Fig. 6-(2)	−72.9823	−1.57
B_4^{++}	3	Fig. 6-(3)	−97.6646	2.07
B_5^{++}	4	Fig. 6-(4)	−122.4083	7.37
B_6^{++}	3	Fig. 6-(5)	−147.2227	14.60

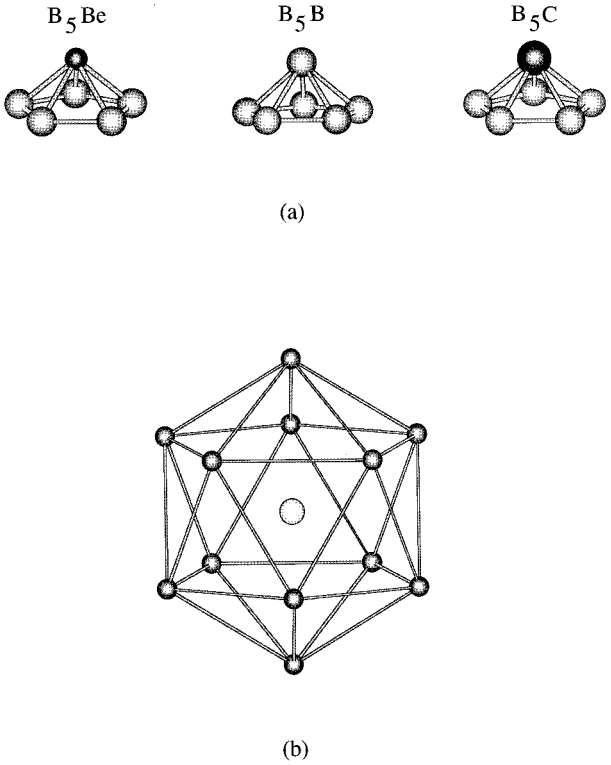

FIG. 7. (a) Equilibrium geometries of B_5X (X=Be, B, C) clusters. (b) Icosahedric geometry of $B_{12}X$ cluster. The X atom (Be, C) is at the center of the icosahedron.

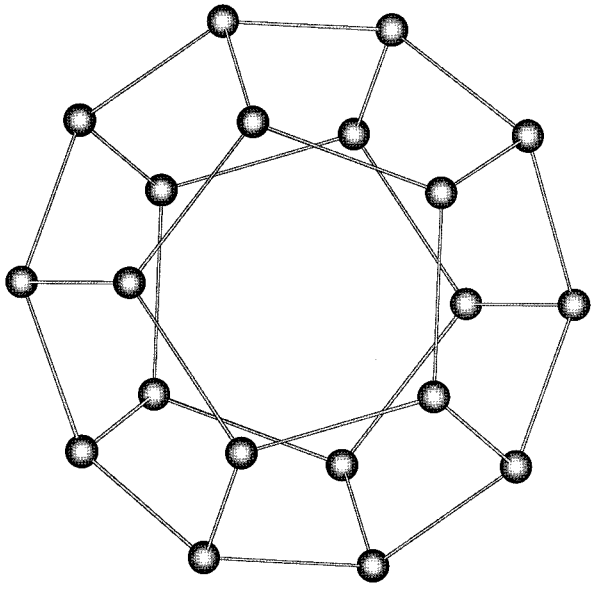

FIG. 8. The dodecahedral geometry of B_{20}.

TABLE X. Energetics, bond lengths (distance of X from B), preferred spin multiplicities, binding energies, and Mulliken charges in boron-rich clusters and B_{20} clusters using B3LYP theory. Note that the Mulliken charge on B represents an average over all B sites.

Type of clusters, B_nX	Total energy, eV	Bond length, Å	Multiplicity	B.E./n, eV	Mulliken charge distribution for B_nX	
					B	X
B_1B	−49.000 497	1.56	3	2.178	0.00	0.00
B_1C	−62.224 208	1.48	4	3.086	0.38	−0.38
B_1Be	−39.016 911	1.88	2	1.071	0.08	−0.08
B_5B	−147.714 168	1.64	1	5.409	0.04	−0.22
B_5C	−160.876 570	1.66	2	5.434	0.05	−0.25
B_5Be	−137.673 035	1.70	2	4.779	0.06	−0.31
B_{12}	−295.337 812	1.78	1	5.204	0.00	0.00
$B_{12}B$	−319.818 887	1.99	2	4.931	0.04	−0.44
$B_{12}C$	−333.083 451	2.05	3	5.156	0.09	−1.06
$B_{12}Be$	−310.075 338	1.83	1	5.263	0.11	−1.34
B_{20}	−492.486 284	2.47	1	5.553	0.00	0.00

electronic bonding in boron clusters is similar to that in boron-rich solids and is characterized by a three-center bond. (4) The geometries of singly charged B_5 and B_6 clusters are significantly different from the corresponding neutral geometries, while in smaller clusters the effect of ionization on geometries is rather minimal. (5) For clusters consisting of fewer than 6 atoms, the fragmentation of B_n^+ proceeds by the emission of a B^+ ion as seen experimentally. (6) The critical size for Coulomb explosion of doubly charged B_n^{++} clusters has not been reached up to $n=6$. (7) The energetics of the compound B_n clusters containing impurities such as Be and C suggest that their relative stabilities depend on cluster size and deviate markedly from what can be expected from a simple jellium model. (8) Contrary to initial expectation, B_{20} does not show any marked stability. This indicates that boron clusters are not stabilized by two-center bonding.

ACKNOWLEDGMENT

This work was supported in part by a research grant from the U.S. Department of Energy (DEFG05-87ER45316).

[1] *Physics and Chemistry of Finite Systems: From Clusters to Crystals*, Vols. I and II, edited by P. Jena, S. N. Khanna, and B. K. Rao (Kluwer, Dordrecht, 1992).
[2] D. Emin, Phys. Today **55** (1987); *Boron Hydride Chemistry*, edited by E. L. Mutterties (Academic, New York, 1975).
[3] S. J. La Placa, P. A. Roland, and J. J. Wynne, Chem. Phys. Lett. **190**, 163 (1992).
[4] S. Becker and H. J. Dietze, Int. J. Mass Spectrom. Ion Processes **73**, 157 (1986).
[5] J. Berkowitz and W. A. Chupka, J. Chem. Phys. **40**, 2735 (1964).
[6] L. Hanley, J. L. Whitten, and S. L. Anderson, J. Phys. Chem. **92**, 5803 (1988).
[7] S. R. Langhoff and C. W. Bauschlicher, J. Chem. Phys. **95**, 5882 (1991).
[8] A. K. Ray, I. A. Howard, and K. M. Kanal, Phys. Rev. B **45**, 14247 (1992).
[9] R. Kawai, M. W. Sung, and J. H. Weare in *Physics and Chemistry of Finite Systems: From Clusters to Crystals*, Vol. I, edited by P. Jena, S. N. Khanna, and B. K. Rao (Kluwer, Dordrecht, 1992), p. 441.
[10] W. J. Hehre, L. Radom, P. v. R. Schleyer, and J. A. Pople, *Ab Initio Molecular Orbital Theory* (Wiley, New York, 1986).
[11] A. D. Becke, Phys. Rev. A **38**, 3098 (1988); A. D. Becke, J. Chem. Phys. **84**, 4524 (1988); J. P. Perdew and Y. Wang, Phys. Rev. B **45**, 13244 (1992) and references therein; A. D. Becke, J. Chem. Phys. **98**, 5648 (1993).
[12] GAUSSIAN 94, Revision B 1, M. J. Frisch, G. W. Trucks, H. B. Schlegel, P. M. W. Gill, B. G. Johnson, M. A. Robb, J. R. Cheeseman, T. Keith, G. A. Petersson, J. A. Montgomery, K. Raghavachari, M. A. Al-Laham, V. G. Zakrzewski, J. V. Ortiz, J. B. Foresman, J. Cioslowski, B. B. Stefanov, A. Nanayakkara, M. Challacombe, C. Y. Peng, P. Y. Ayala, W. Chen, M. W. Wong, J. L. Andres, E. S. Replogle, R. Gomperts, R. L. Martin, D. J. Fox, J. S. Binkley, D. J. Defrees, J. Baker, J. P. Stewart, M. Head-Gordon, C. Gonzalez, and J. A. Pople, Gaussian, Inc., Pittsburgh PA, 1995.
[13] A. E. Douglas and G. Herzberg, Can. J. Res. Sect. A **18**, 165 (1940).
[14] C. F. Bender and E. R. Davidson, J. Chem. Phys. **46**, 3313 (1967).
[15] M. Dupuis and B. Liu, J. Chem. Phys. **68**, 2902 (1978).
[16] P. J. Bruna and J. S. Wright, J. Phys. Chem. **94**, 1774 (1990).
[17] K. Sattler, J. Mühlbach, O. Echt, P. Pfau, and E. Recknagel, Phys. Rev. Lett. **47**, 160 (1981); B. K. Rao, P. Jena, M. Manninen, and R. H. Nieminen, Phys. Rev. Lett. **58**, 1188 (1987).
[18] F. Liu, M. R. Press, S. N. Khanna, and P. Jena, Phys. Rev. Lett. **59**, 2562 (1987).
[19] T. T. Tsong, Surf. Sci. **177**, 593 (1986).
[20] S. N. Khanna and P. Jena, Phys. Rev. B **51**, 13705 (1995).